



Ultralow-power dielectric-modulated nanogap-embedded sub-20-nm TGRC-MOSFET for biosensing applications

Ajay Kumar¹ · M. M. Tripathi¹ · Rishu Chaujar²

Published online: 11 September 2018
© Springer Science+Business Media, LLC, part of Springer Nature 2018

Abstract

This work examines a transparent gate recessed channel (TGRC) metal–oxide–semiconductor field-effect transistor (MOSFET) for biosensing, including a nanogap cavity for detection of biomolecules and a transparent gate to enhance the overall current efficiency of the RC-MOSFET. For the detection of neutral biomolecules, electrical characteristics such as I_{ON}/I_{OFF} , shift in threshold voltage and change in surface potential have been studied and thereafter, sensitivity of has been evaluated. The biosensor showed enhanced sensitivity for biomolecules with increase in their dielectric value, due to greater on-current owing to the change in capacitances. The capacitances were therefore also evaluated. In addition, immobilization of biomolecules degrades the noise immunity of MOSFET and thereby their overall biosensing performance, while the noise immunity of the TGRC device was very high even in the presence of biomolecules. Furthermore, modulation of the cavity gap length was also investigated, revealing that its increase (from 8 to 20 nm) significantly enhanced the sensitivity of the proposed biosensor. Overall, the results of this analysis reveal that such TGRC-MOSFET biosensors can exhibit high sensitivity (1.45) at very low drain bias (0.2 V), enabling their use for biosensor applications to diagnose various diseases which require lower noise, high speed, low power, and high density.

Keywords Biosensor · Dielectric constant · ITO · Nanogap · Sensitivity · TGRC-MOSFET

1 Introduction

With the aid of nanotechnology, various kinds of biosensor have been developed for use in medical applications and disease diagnostics, which require high performance. According to medical science, prompt detection of any disease, mainly cancer, favors patient survival. Numerous methods have been developed for detection of biomolecules, e.g., the enzyme-linked immunosorbent assay [1], for Alzheimer's disease, ovarian cancer, and coronary artery disease. However, many of these approaches are complicated and time-consuming due

to the requirement for labeling techniques [2]. Field-effect transistor (FET)-based biosensors have attracted much attention over recent years owing to their good scalability, high sensitivity, rapid electrical detection, low power consumption, direct electrical readout, and low-cost mass production in comparison with other methods such as surface plasmon resonance devices [3], microcantilevers [4], and arrays of fluorescence sensors [5]. Low-cost, highly sensitive, reliable, user-friendly, and quick diagnostic biosensing devices are essential for different biological and biomedical applications [6]. For biosensing applications, sensitivity is the key factor for a MOSFET. Over time, various structures such as the nanowire junctionless MOSFET [7] and tunnel FET [8, 9] have been introduced to enhance the sensitivity of FET-based biosensors. Nanotechnology-based biosensor devices have also been used [10–12] to overcome the difficulties of conventional health diagnostic methods.

Moreover, advanced development of semiconductor technology for medical applications has shrunk device dimensions to the nanoscale regime to provide high packing density for high-speed integrated circuits. However, in such ultra-scaled device, the influence of short-channel effects (SCEs)

✉ Rishu Chaujar
chaujar.rishu@dtu.ac.in

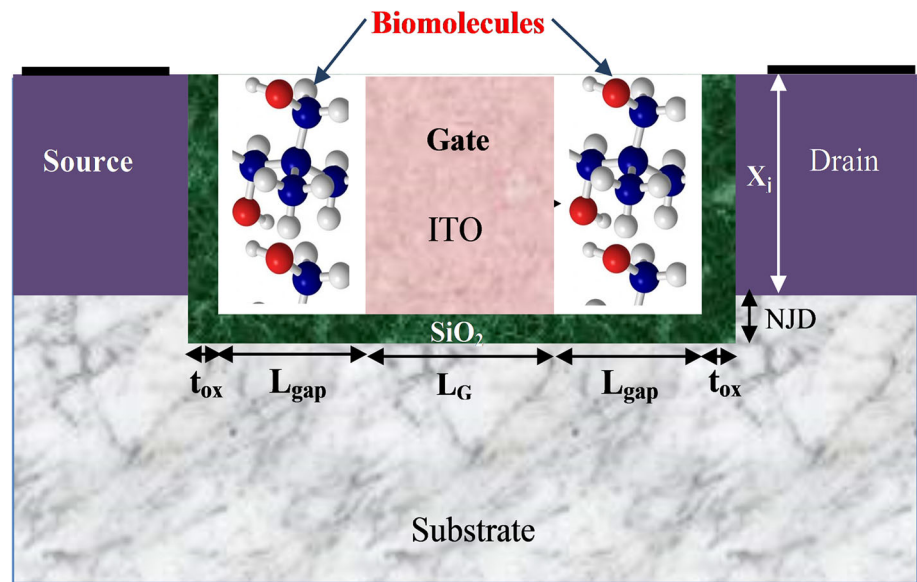
Ajay Kumar
ajaykumar@dtu.ac.in

M. M. Tripathi
mmtripathi@dce.ac.in

¹ Department of Electrical Engineering, Delhi Technological University, Delhi 110042, India

² Department of Applied Physics, Delhi Technological University, Delhi 110042, India

Fig. 1 Schematic structure of the TGRC-MOSFET biosensor



deeply affects device performance [7]. To overcome SCEs, several device engineering schemes and alternative device structures have been reported in literature [13–18]. Among these, the recessed channel (RC) MOSFET is considered to be the most promising, since it overcomes almost all the SCEs and is also compatible with recent complementary metal–oxide–semiconductor (CMOS) technology [19]. Numerous innovative gate materials have been explored recently to enhance the current driving capability of CMOS devices while enhancing their overall performance. In the proposed (TGRC-MOSFET) biosensor device, indium-doped tin oxide (ITO) has been used as a gate material, due to its enhanced electrical properties, as demonstrated in previous work [20–25]. Use of ITO significantly enhances the on-current, due to its very low resistivity ($10^{-5} \Omega \text{ cm}$) and high mobility ($53.5 \text{ cm}^2 \text{ V}^{-1} \text{ s}^{-1}$) [26].

In the work presented herein, a TGRC-MOSFET for use as a biosensor was simulated, considering the electrical properties of various biomolecules. The main use of biosensors is to sense biological elements, based on their sensitivity to and binding specificity of biological species such as enzymes, proteins, nucleotides, or antibodies. In the proposed TGRC-MOSFET biosensor, the channel potential of the device is influenced by the electrical properties of the biomolecules, enabling their detection. In a conventional MOSFET, current flows in the channel when the gate voltage exceeds a threshold voltage (V_{TH}). In a biosensor, this effect is modulated by the dielectric constant due to immobilization of biomolecules below the gate electrode, because the threshold voltage depends upon the gate capacitance. Absorption of biomolecules therefore affects the electrical characteristics of the sensor, changing its sensitivity.

2 Device structure, simulation methodology, and calibration

The three-dimensional (3D) structure of the considered biosensor device is shown in Fig. 1. For immobilization of biomolecules, a small nanocavity is created in the gate insulator region, since this is the most important region determining the behavior and characteristics of a CMOS device. Here, L_{gap} is the length of the nanogap cavity (8 nm), t_{ox} is the oxide thickness (2 nm), and the gate length L_G is taken to be 20 nm. The source and drain regions are highly doped with n -type impurity to $5 \times 10^{19} \text{ cm}^{-3}$, while the substrate is doped with p -type impurity to $1 \times 10^{17} \text{ cm}^{-3}$, as shown in Fig. 1. The negative junction depth (NJD) is taken to be 10 nm, while the gate workfunction of ITO (Φ_{ITO}) is 4.7 eV. The gate bias (V_{gs}) is 0.7 V and the drain bias (V_{ds}) is 0.2 V throughout the analysis, unless otherwise stated. Absorption of different biomolecules is modeled by introduction of an insulator having the same dielectric constant as a particular biomolecule into the nanogap cavity. The unfilled cavity (i.e., with no biomolecules present) is modeled by using an insulator with dielectric constant $k = 1$, while the dielectric constant of the different considered biomolecules is as follows: streptavidin ($k = 2.1$) [27], biotin ($k = 2.63$) [28], 3-aminopropyltriethoxysilane (APTES) ($k = 3.57$), and protein ($k = 8$) [29]. Streptavidin–biotin is used to detect Marek’s disease virus (MDV) using an enzyme-linked immunosorbent assay (ELISA) method [30], while APTES facilitates immobilization of biomolecules onto the surface for detection of dengue virus [31].

ATLAS is a powerful simulation tool that can be used for extraction of reliability results and figures of merit (FOMs) [32]. Various simulation models were applied in this work, including the Lombardi constant voltage and temperature

Fig. 2 Calibrated **a** output and **b** transfer characteristics of experimental and simulation data for a recessed channel MOSFET (with 36 nm gate length)

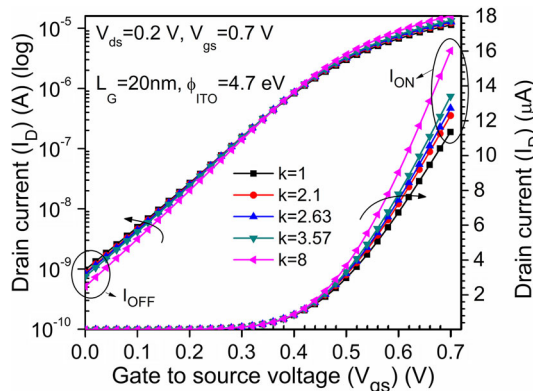
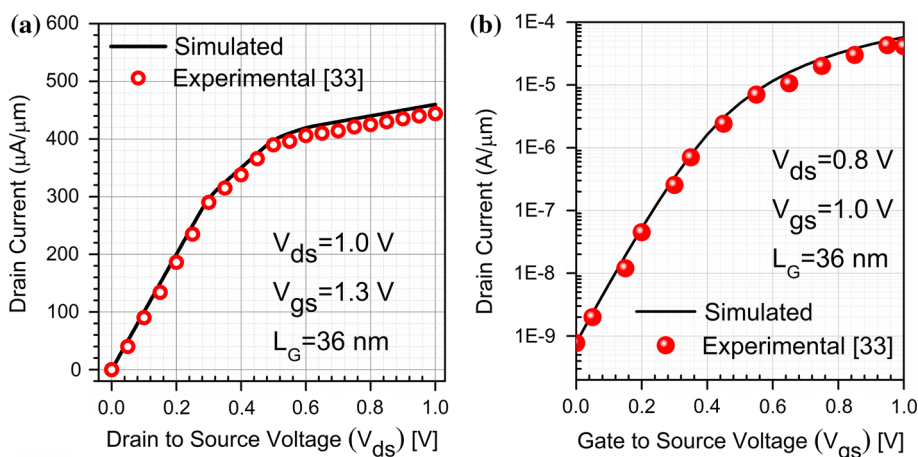


Fig. 3 Transfer characteristics of the nanogap-embedded TGRC-MOSFET in the presence of different biomolecules

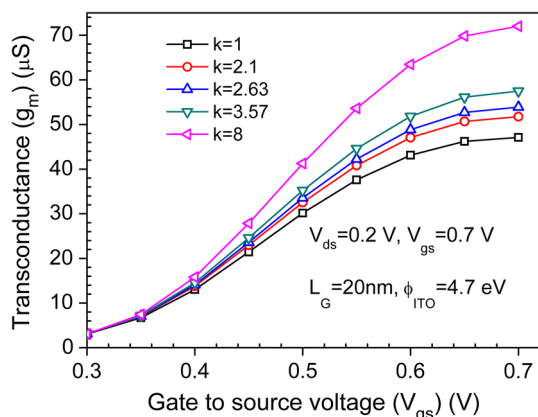


Fig. 4 Transconductance (g_m) of the nanogap-embedded TGRC-MOSFET in the presence of different biomolecules

(CVT) model to consider all the mobilities, e.g., due to scattering caused by the parallel and perpendicular fields applied on the device. For carrier generation–recombination, we used Shockley–Read–Hall (SRH) recombination. Fermi–Dirac statistics were used in case of very highly doped material. To include information about the low energy (temperature) of the carriers, we used the energy balance transport

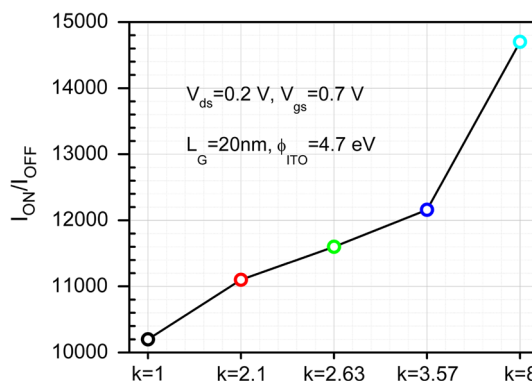


Fig. 5 Switching ratio (I_{on}/I_{off}) of the TGRC-MOSFET at drain voltage of 0.2 V in the presence of different biomolecules

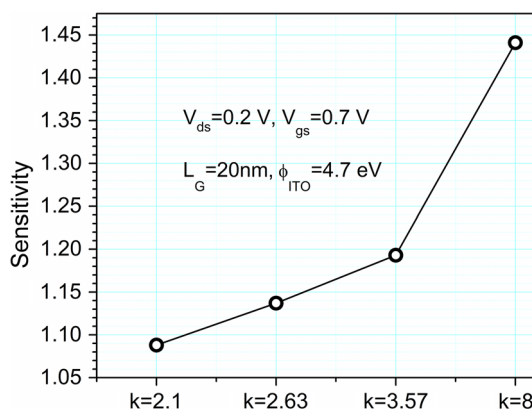


Fig. 6 Sensitivity of the TGRC-MOSFET at drain voltage of 0.2 V to different biomolecules

(EBT) model [32]. Calibration of the physical model parameters of the simulated device against experimental results by Appenzeller et al. [33] is shown in Fig. 2. To validate the simulation results, output and transfer characteristic statistics were extracted [33] for a 36-nm RC-MOSFET, as shown in Fig. 2a and b, respectively. The simulation results in Fig. 2a, b almost match with the experimental data for a sub-40-nm RC MOSFET, thus validating the simulation model.

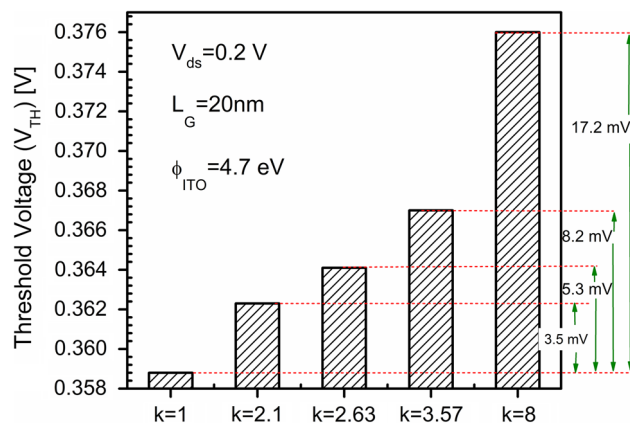
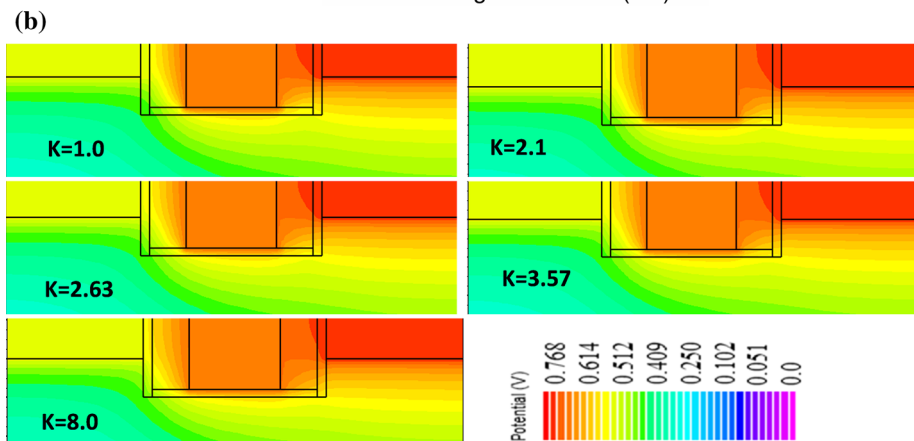
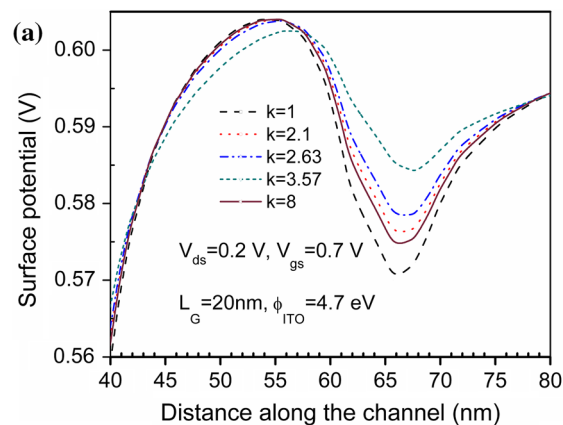


Fig. 7 Threshold voltage shifts for the TGRC-MOSFET in the presence of different biomolecules

3 Results and discussion

It can be observed from the transfer characteristics of the biosensor (Fig. 3) that, when neutral biomolecules are immobilized ($k > 1$) in the cavity, the on-current is significantly enhanced compared with in their absence ($k = 1$), owing to the increase in the dielectric constant and thus transconductance (Fig. 4). Different biomolecules can be detected based on the measured current [5]. Due to the increase in the

Fig. 8 a Surface potential along the channel from the source to drain and **b** corresponding contour plots of the TGRC-MOSFET in the presence of different biomolecules with $k = 1, 2.1, 2.63, 3.57,$ and 8



on-current, the switching ratio (I_{on}/I_{off}) also increases with the dielectric value, as shown in Fig. 5. Thus, the change in the drain current or the enhancement in I_{on} and the switching ratio for a particular biomolecule could be used as key parameters for their detection/sensing. Furthermore, sensitivity is one of the critical parameters for the proposed biosensor device. In this work, the sensitivity (S) is defined as

$$S = \frac{I_{on}(k > 1)}{I_{on}(k = 1)}. \quad (1)$$

Figure 6 presents the sensitivity for the different biomolecules, clearly showing a higher value for protein biomolecules ($k = 8$) compared with streptavidin, biotin, and APTES (2.1, 2.63, and 3.57, respectively); note that the use of a uniform dielectric value implies that the cavity is completely filled by the specific biomolecule.

The threshold voltage was used as a sensing parameter for detection, being directly related to the dielectric constant; in this work, the threshold voltage is defined as the gate voltage at which the drain current is equal to 10^{-7} A/ μ m. The threshold voltage increases as the dielectric constant of the biomolecule is increased, as shown for the TGRC-MOSFET in Fig. 7. Threshold voltage shifts (ΔV_{TH}) of 3.5 mV, 5.3 mV, 8.2 mV, and 17.2 mV are observed when the dielectric constant changes from the unfilled cavity to a cavity filled with

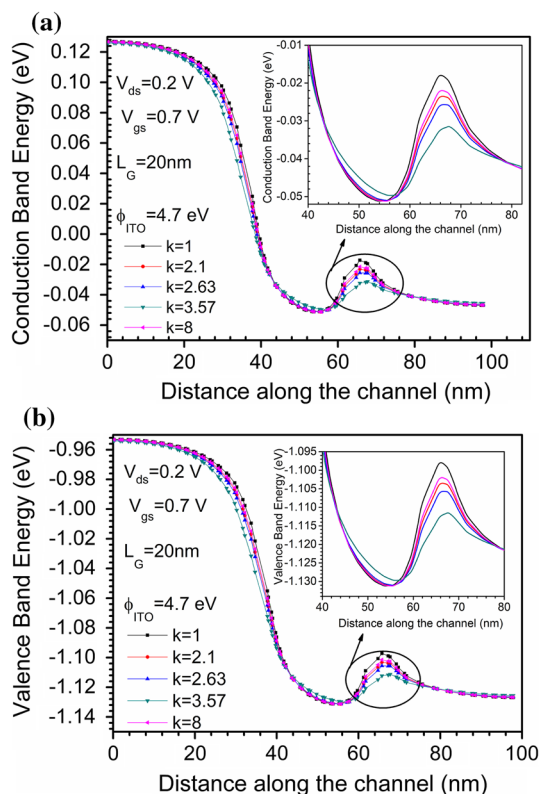


Fig. 9 Effect on **a** conduction band and **b** valence band along the channel of the TGRC-MOSFET in the presence of different biomolecules

biomolecules having $k = 2.1, 2.63, 3.57,$ and 8 (Fig. 7). The threshold voltage shift (ΔV_{TH}) can also be used to define the sensitivity of the biosensor as $\Delta V_{TH} = V_{TH}(\text{after absorption of the molecule}) - V_{TH}(\text{air-filled cavity})$ [34, 35]. The

threshold voltage shift is directly proportional to the permittivity of the absorbed neutral biomolecule, i.e.,

$$\Delta V_{TH} \propto k_{bio}. \tag{2}$$

Thus, it can be said that, the higher the absolute value of ΔV_{TH} , the better the sensitivity of the biosensor, as ΔV_{TH} also represents the sensitivity of the device and the threshold voltage shifts toward higher gate voltage in the presence of biomolecules in the nanogap cavity [7].

In addition, the electrical performance of the TGRC-MOSFET biosensor was also examined in terms of the surface potential (Fig. 8a). Under the cavity region, deformation of the potential occurs (especially at the drain end). When biomolecules are immobilized in the cavity, a change in potential is observed due to the change in the dielectric constant due to the biomolecules. This shift in potential can also be used to detect the presence of biomolecules in the cavity region. The contour plots of the surface potential in Fig. 8b clearly reveal the change in potential when biomolecules are immobilized in the nanocavity.

Figure 9a, b shows the energy band profile [36] in terms of the conduction- and valence-band energies. When biomolecules are immobilized in the nanogap cavity, these values clearly change. The shift in the energy band is more prominent for the biomolecule with dielectric constant of 3.57 but less prominent for protein, streptavidin, and biotin, in comparison with the case of no biomolecules [37], as reflected in Fig. 9a, b. Thus, the TGRC device can also be used as a low-power sensing device due to this effective change in the energy band profiles at low drain bias (0.2 V) for different biomolecules. Moreover, it is also observed from Fig. 10a that, in the presence of various biomolecules ($k =$

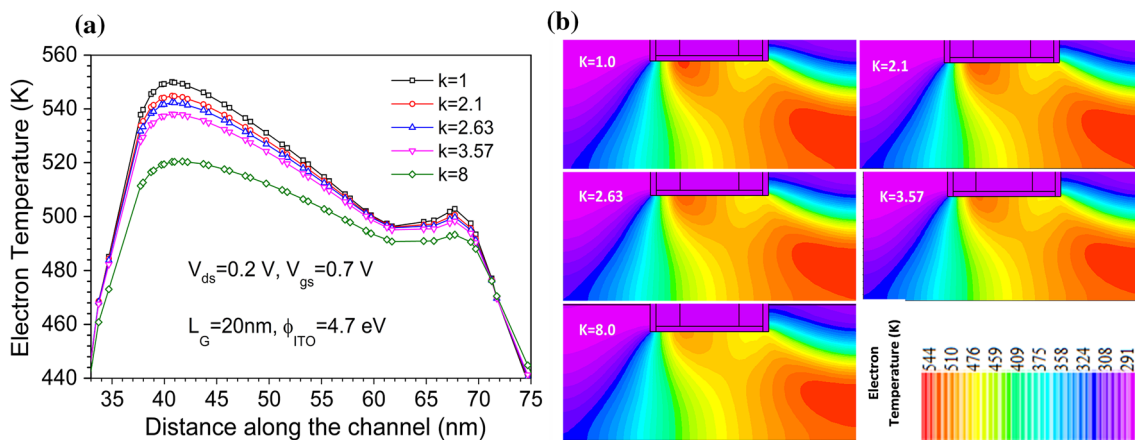


Fig. 10 **a** Electron temperature along the channel from the source to drain and **b** corresponding contour plots for the TGRC-MOSFET in the presence of different biomolecules

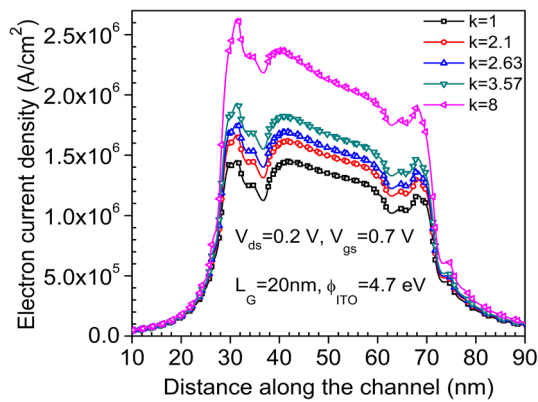


Fig. 11 Electron current density along the channel from the source to drain of the TGRC-MOSFET in the presence of different biomolecules

2.1 to $k = 8$), the electron temperature decreases (~ 510 K) due to the high- k dielectric (biomolecules) in the nanocavity gap, due to which leakage currents such as hot-electron injected gate current and impact-ionization substrate current are almost eliminated, thereby enhancing the I_{on} (shown in Fig. 2) and sensitivity of the device. The contour plots

in Fig. 10b clearly show how the temperature varies when biomolecules are introduced into the nanogap cavity. This change in temperature with the dielectric constant can also be used to detect/sense which biomolecules are present.

Furthermore, the electron current density [38] in the presence and absence of different biomolecules in the nanocavity gap was also investigated (Fig. 11). For the proposed biosensor, it is evident that the electron current density is very low when the nanocavity gap is unfilled (for air, $k = 1$) but increases when the nanocavity gap is filled with different biomolecules, in increasing order of dielectric constant. For higher current density, I_{on} will also be high, due to which the switching ratio is increased. Thus, the device will be more sensitive when the nanocavity gap is filled with biomolecules, and this effect will increase with their dielectric constant (as shown in Fig. 6). It is also observed from Fig. 11 that the electron current density is higher just below the nanocavity gap.

3.1 Effect on parasitic capacitances

The presence of biomolecules can easily be observed via the change in stray capacitances, as the stray (parasitic) capaci-

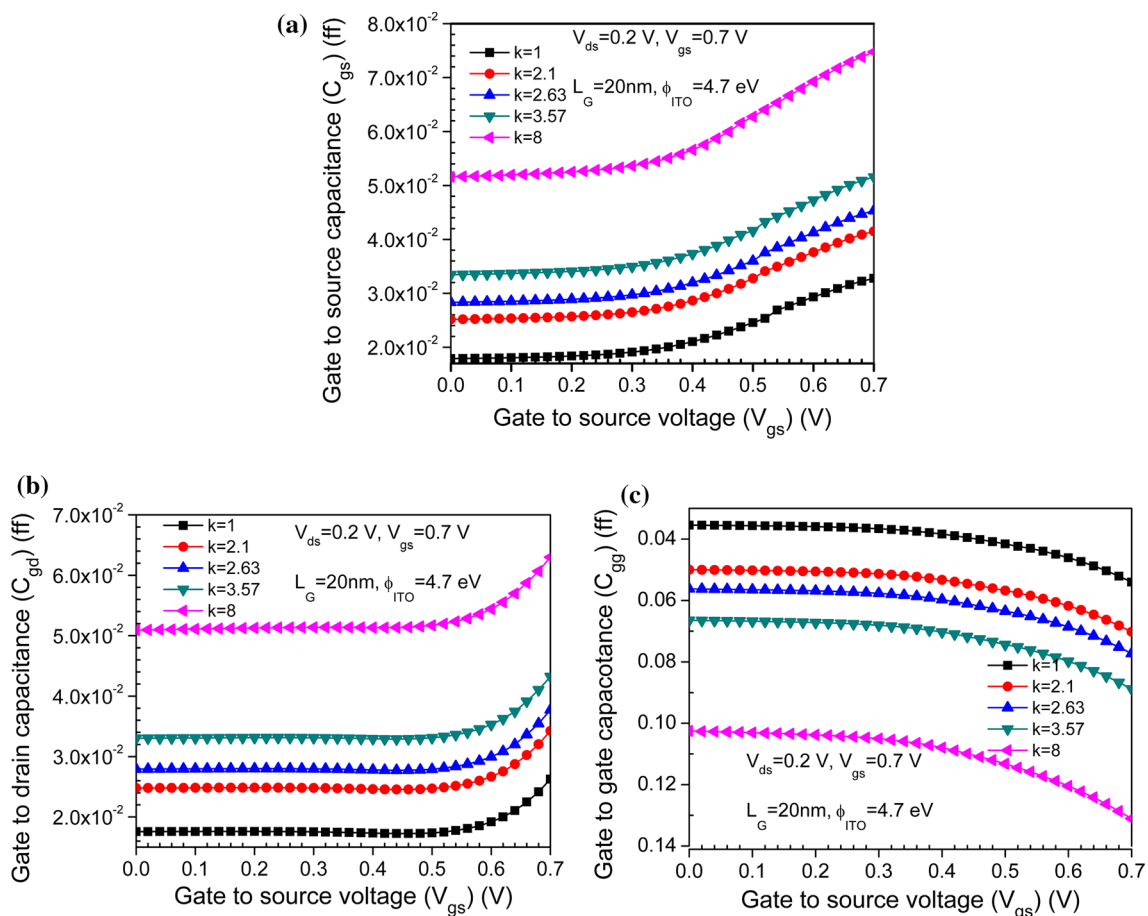


Fig. 12 Effect of different biomolecules on the parasitic capacitances **a** C_{gs} , **b** C_{gd} , and **c** C_{gg} of the TGRC-MOSFET

tances of a field-effect transistor are altered when changing the dielectric constant of the gate oxide. Figure 12a shows that the gate-to-source capacitance (C_{gs}) and gate-to-drain capacitance (C_{gd}) are altered (increased) when changing (increasing) the dielectric constant to $k = 2.1, 2.63, 3.57,$ and $8,$ in comparison with the unfilled nanogap. When V_{gs} increases, the accumulation of charge carriers near the gate increases [39], and as a result, the gate-to-source capacitance and gate-to-drain capacitance also increase. Similarly, the gate capacitance (C_{gg}) is altered in the presence of biomolecules with different dielectric constants, and when V_{gs} increases, the accumulation of charges at the gate increases, and thus so does the gate capacitance [39], as shown in Fig. 12c. When molecules with higher dielectric constant are immobilized, these changes in the capacitances become more prominent, as is evident from Fig. 12a–c. These parasitic capacitances must be as low as possible in semiconductor devices for use in high-performance applications. According to these results, all the parasitic capacitances ($C_{gs}, C_{gd},$ and C_{gg}) evaluated in the presence of different biomolecules were very low (on femtofarad scale).

3.2 Noise assessment

In the presence of any external agent (e.g., biomolecules) in the channel region of a CMOS device, the electrical behavior in terms of the I – V characteristics is altered. Such shifts in the I – V characteristics and other electrical behaviors can be used as key parameters for detection of biomolecules, as clearly shown above. However, the presence of such agents can also sometimes lead to noise, which degrades biosensor performance. Therefore, to examine the noise immunity of the proposed biosensor, noise FOMs such as the minimum noise figure, noise conductance, etc. were also evaluated w.r.t. frequency [14]. As is clear from Figs. 13, 14, and 15, when biomolecules are immobilized in the cavity, all the noise parameters improved significantly at high frequency. This observation can mainly be attributed to the transparent conducting material (ITO) used in the TGRC-MOSFET architecture, because the random motion of free electrons is decreased in such materials. In a transparent conducting material, the temperature (Fig. 10) does not increase significantly when the concentration of charge carriers is increased, thereby improving the noise immunity of the TGRC biosensor in the presence of biomolecules. Furthermore, Fig. 15 shows another noise parameter, called the optimum source impedance ($Z_{OPT} = R_{OPT} + jX_{OPT}$), with respect to frequency for the different biomolecules, being nearly zero at higher frequencies when the nanocavity gap is empty but increasing with the dielectric constant of the biomolecule. This indicates that the device exhibits very low noise in the presence of biomolecules and is thus suitable for use in biosensing applications.

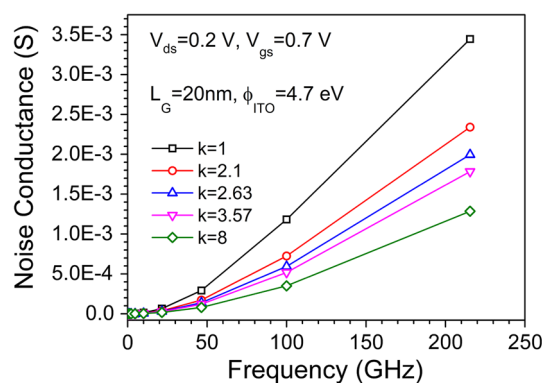


Fig. 13 Noise conductance in the GHz frequency range for the TGRC-MOSFET in the presence of different biomolecules

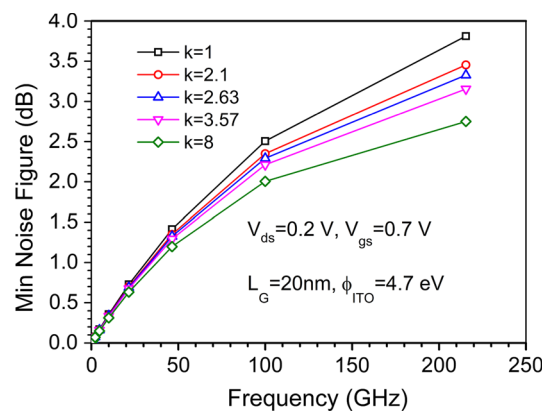


Fig. 14 Minimum noise figure in the GHz frequency range for the TGRC-MOSFET in the presence of different biomolecules

3.3 Effect of the nanogap cavity length

Moreover, the length of the cavity (L_{gap}) [36] was also varied, with the aim of determining its effect on the sensitivity and thereby the performance of the biosensor. Figure 16 shows that, with increase in the cavity gap length, the on/off ratio was evidently reduced due to an increase in the off-current

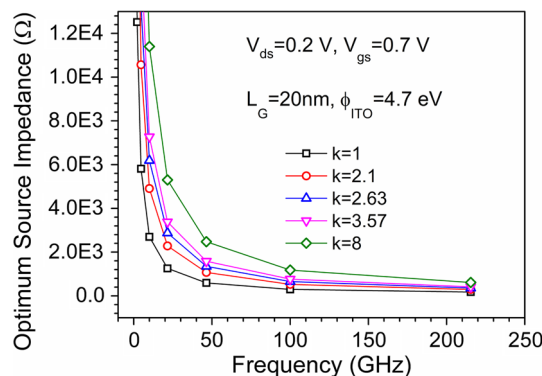


Fig. 15 Optimum source impedance in the GHz frequency range for the TGRC-MOSFET in the presence of different biomolecules

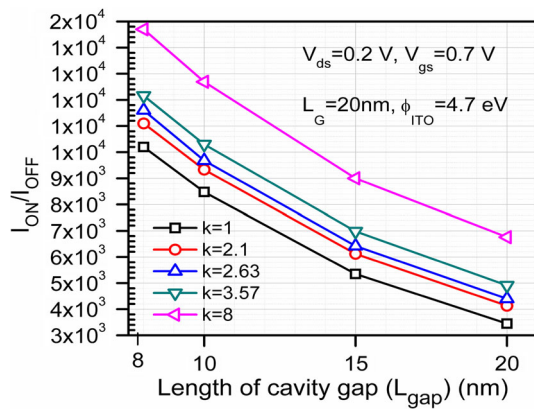


Fig. 16 Effect of varying the cavity gap length in the TGRC-MOSFET on the switching ratio for different biomolecules

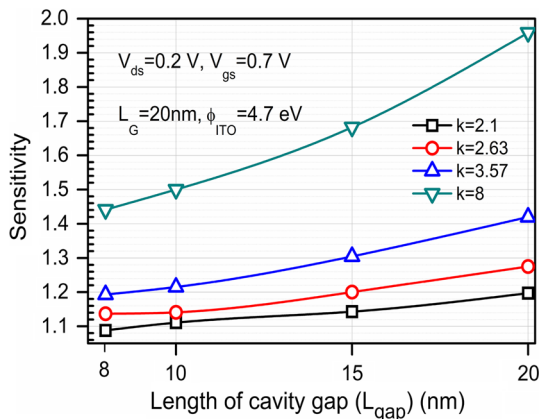


Fig. 17 Effect of varying the cavity gap length in the TGRC-MOSFET on the sensitivity for different biomolecules

resulting from higher capacitance. Moreover, the sensitivity of the TGRC biosensor with different cavity gap lengths was also evaluated, revealing that it increased significantly with increase in L_{gap} (Fig. 17). From this figure, it is observed that the sensitivity increased with k for given L_{gap} . Thus, for $L_{\text{gap}} = 20$ nm, the nanogap-embedded TGRC biosensor showed better sensitivity for protein ($k = 8$) in comparison with the other biomolecules. Figure 18 shows the change in the threshold voltage with L_{gap} (from 8 to 20 nm) for the different biomolecules; this noticeable change in the threshold voltage with the dielectric constant can be used as one of the sensing parameters for detection of biomolecules. Thus, the TGRC-MOSFET with cavity gap length of 20 nm showed optimum performance and hence could be employed as a low-power, high-sensitivity biosensor for diagnosis of various associated diseases.

4 Conclusions

The applicability of a nanogap-embedded ITO-gated recessed channel MOSFET as a biosensor was investigated.

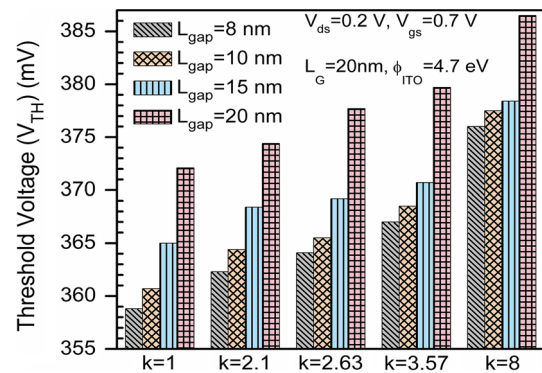


Fig. 18 Effect of varying the cavity gap length in the TGRC-MOSFET on the threshold voltage for different biomolecules

For detection of various biomolecules, the electrical behavior was studied in terms of the threshold voltage shift, sensitivity, switching ratio, surface potential, capacitance, and noise FOMs. The results obtained clearly show that, due to the ITO gate in the nanogap cavity, the electrical performance of the TGRC biosensor was significantly enhanced, showing higher sensitivity for biomolecules with high dielectric value. It was found that the sensitivity was higher for detection of protein ($k \approx 8$) in comparison with the other biomolecules, with higher noise immunity. Such TGRC-MOSFET biosensors are therefore proved to be favorable devices for use in sensing applications, due to their high sensitivity and low-power electrical detection of different biomolecules. Furthermore, the effects of the cavity gap length on the switching ratio, V_{TH} , and sensitivity of the proposed biosensor were also examined, revealing that the sensitivity increased with increase in the cavity length while the overall biosensor performance was slightly degraded. Therefore, the cavity gap length must be optimized for better performance, which will enable use of such sub-20-nm TGRC-MOSFETs as low-noise, high-speed, high-sensitivity biosensors for detection of various associated diseases.

Acknowledgements The authors are grateful to the University Grants Commission (UGC) for provision of financial assistance to carry out this work.

References

- Comini, E., Baratto, C., Concina, I., Faglia, G., Falasconi, M., Ferroni, M., Galstyan, V., Gobbi, E., Ponzoni, A., Vomiero, A., Zappa, D., Sberveglieri, V., Sberveglieri, G.: Metal oxide nanoscience and nanotechnology for chemical sensors. *Sens. Actuators B Chem.* **179**, 3–20 (2013)
- Lee, J., Jang, J., Choi, B., Yoon, J., Kim, J.-Y., Choi, Y.-K., Kim, D.M., Kim, D.H., Choi, S.-J.: A highly responsive silicon nanowire/amplifier MOSFET hybrid biosensor. *Sci. Rep.* **5**, 12286 (2015)

3. Bergveld, P.: The development and application of FET-based biosensors. *Biosensors* **2**(1), 15–33 (1986)
4. Sang, S., Wang, Y., Feng, Q., Wei, Y., Ji, J., Zhang, W.: Progress of new label-free techniques for biosensors: a review. *Crit. Rev. Biotechnol.* **36**(3), 465–481 (2016)
5. Im, H., Huang, X.-J., Gu, B., Choi, Y.-K.: A dielectric-modulated field-effect transistor for biosensing. *Nat. Nanotechnol.* **2**(7), 430–434 (2007)
6. Vu, X.T., Eschermann, J.F., Stockmann, R., GhoshMoulick, R., Offenhäusser, A., Ingebrandt, S.: Top-down processed silicon nanowire transistor arrays for biosensing. *Phys. Status Solidi* **206**(3), 426–434 (2009)
7. Ahangari, Z.: Performance assessment of dual material gate dielectric modulated nanowire junctionless MOSFET for ultrasensitive detection of biomolecules. *RSC Adv.* **6**(92), 89185–89191 (2016)
8. Chandan, B.V., Nigam, K., Sharma, D.: Junctionless based dielectric modulated electrically doped tunnel FET based biosensor for label-free detection. *Micro Nano Lett.* **13**(4), 452–456 (2018)
9. Kanungo, S., Chattopadhyay, S., Gupta, P.S., Sinha, K., Rahaman, H.: Study and analysis of the effects of SiGe source and pocket-doped channel on sensing performance of dielectrically modulated tunnel FET-based biosensors. *IEEE Trans. Electron Devices* **63**(6), 2589–2596 (2016)
10. Azmi, M.M., Tehrani, Z., Lewis, R., Walker, K.-A., Jones, D., Daniels, D., Doak, S., Guy, O.: Highly sensitive covalently functionalised integrated silicon nanowire biosensor devices for detection of cancer risk biomarker. *Biosens. Bioelectron.* **52**, 216–224 (2014)
11. Ahn, J.-H., Choi, S.-J., Han, J.-W., Park, T.J., Lee, S.Y., Choi, Y.-K.: Double-gate nanowire field effect transistor for a biosensor. *Nano Lett.* **10**(8), 2934–2938 (2010)
12. Gao, A., Lu, N., Dai, P., Li, T., Pei, H., Gao, X., Gong, Y., Wang, Y., Fan, C.: Silicon-nanowire-based CMOS-compatible field-effect transistor nanosensors for ultrasensitive electrical detection of nucleic acids. *Nano Lett.* **11**(9), 3974–3978 (2011)
13. Barsan, R.M.: Analysis and modeling of dual-gate MOSFET's. *IEEE Trans. Electron Devices* **28**(5), 523–534 (1981)
14. Gupta, N., Chaujar, R.: Influence of gate metal engineering on small-signal and noise behaviour of silicon nanowire MOSFET for low-noise amplifiers. *Appl. Phys. A* **122**(8), 1–9 (2016)
15. Gupta, N., Chaujar, R.: Optimization of high-k and gate metal workfunction for improved analog and intermodulation performance of gate stack (GS)-GEWE-SiNW MOSFET. *Superlattices Microstruct.* **97**, 630–641 (2016)
16. Gupta, N., Chaujar, R.: Investigation of temperature variations on analog/RF and linearity performance of stacked gate GEWE-SiNW MOSFET for improved device reliability. *Microelectron. Reliab.* **64**, 235–241 (2016)
17. Gupta, N., Kumar, A., Chaujar, R.: Oxide bound impact on hot-carrier degradation for gate electrode workfunction engineered (GEWE) silicon nanowire MOSFET. *Microsyst. Technol.* **22**, 2655–2664 (2015)
18. Chaujar, R., Kaur, R., Saxena, M., Gupta, M., Gupta, R.: TCAD assessment of gate electrode workfunction engineered recessed channel (GEWE-RC) MOSFET and its multilayered gate architecture—part I: hot-carrier-reliability evaluation. *IEEE Trans. Electron Devices* **55**(10), 2602–2613 (2008)
19. Chaujar, R., Kaur, R., Saxena, M., Gupta, M., Gupta, R.: Laterally amalgamated DUAL material GATE concave (L-DUMGAC) MOSFET for ULSI. *Microelectron. Eng.* **85**(3), 566–576 (2008)
20. Kumar, A., Gupta, N., Chaujar, R.: Analysis of novel transparent gate recessed channel (TGRC) MOSFET for improved analog behaviour. *Microsyst. Technol.* **22**(11), 2665–2671 (2016)
21. Kumar, A., Gupta, N., Chaujar, R.: Power gain assessment of ITO based transparent gate recessed channel (TGRC) MOSFET for RF/wireless applications. *Superlattices Microstruct.* **91**, 290–301 (2016)
22. Kumar, A., Gupta, N., Chaujar, R.: TCAD RF performance investigation of transparent gate recessed channel MOSFET. *Microelectron. J.* **49**, 36–42 (2016)
23. Kumar, A., Gupta, N., Chaujar, R.: Effect of structured parameters on the hot-carrier immunity of transparent gate recessed channel (TGRC) MOSFET. *Microsyst. Technol.* **23**, 4057–4064 (2017)
24. Kumar, A., Tripathi, M., Chaujar, R.: Reliability issues of In₂O₅Sn gate electrode recessed channel MOSFET: impact of interface trap charges and temperature. *IEEE Trans. Electron Devices* **65**, 860–866 (2018)
25. Kumar, A., Tripathi, M., Chaujar, R.: In₂O₅ Sn based transparent gate recessed channel MOSFET: RF small-signal model for microwave applications. *AEU-Int. J. Electron. Commun.* (2018)
26. Minami, T.: Transparent conducting oxide semiconductors for transparent electrodes. *Semicond. Sci. Technol.* **20**(4), S35 (2005)
27. Busse, S., Scheumann, V., Menges, B., Mittler, S.: Sensitivity studies for specific binding reactions using the biotin/streptavidin system by evanescent optical methods. *Biosens. Bioelectron.* **17**(8), 704–710 (2002)
28. Densmore, A., Xu, D.-X., Janz, S., Waldron, P., Mischki, T., Lopinski, G., Delâge, A., Lapointe, J., Cheben, P., Lamontagne, B.: Spiral-path high-sensitivity silicon photonic wire molecular sensor with temperature-independent response. *Opt. Lett.* **33**(6), 596–598 (2008)
29. Kim, S., Baek, D., Kim, J.-Y., Choi, S.-J., Seol, M.-L., Choi, Y.-K.: A transistor-based biosensor for the extraction of physical properties from biomolecules. *Appl. Phys. Lett.* **101**(7), 073703 (2012)
30. Davidson, I., Malkinson, M., Strenger, C., Becker, Y.: An improved ELISA method, using a streptavidin-biotin complex, for detecting Marek's disease virus antigens in feather-tips of infected chickens. *J. Virol. Methods* **14**(3–4), 237–241 (1986)
31. Zhang, G.-J., Zhang, L., Huang, M.J., Luo, Z.H.H., Tay, G.K.I., Lim, E.-J.A., Kang, T.G., Chen, Y.: Silicon nanowire biosensor for highly sensitive and rapid detection of Dengue virus. *Sens. Actuators B Chem.* **146**(1), 138–144 (2010)
32. Silvaco, I.: ATLAS User's Manual, Santa Clara, CA, Ver 5 (2011)
33. Appenzeller, J., Martel, R., Avouris, P., Knoch, J., Scholvin, J., del Alamo, J.A., Rice, P., Solomon, P.: Sub-40 nm SOI V-groove n-MOSFETs. *IEEE Electron Device Lett.* **23**(2), 100–102 (2002)
34. Kannan, N., Kumar, M.J.: Dielectric-modulated impact-ionization MOS transistor as a label-free biosensor. *IEEE Electron Device Lett.* **34**(12), 1575–1577 (2013)
35. Choi, J.-M., Han, J.-W., Choi, S.-J., Choi, Y.-K.: Analytical modeling of a nanogap-embedded FET for application as a biosensor. *IEEE Trans. Electron Devices* **57**(12), 3477–3484 (2010)
36. Abdi, D.B., Kumar, M.J.: Dielectric modulated overlapping gate-on-drain tunnel-FET as a label-free biosensor. *Superlattices Microstruct.* **86**, 198–202 (2015)
37. Kranti, A., Armstrong, G.A.: Engineering source/drain extension regions in nanoscale double gate (DG) SOI MOSFETs: analytical model and design considerations. *Solid-State Electron.* **50**(3), 437–447 (2006)
38. Stern, E., Vacic, A., Reed, M.A.: Semiconducting nanowire field-effect transistor biomolecular sensors. *IEEE Trans. Electron Devices* **55**(11), 3119–3130 (2008)
39. Kumar, A., Tripathi, M., Chaujar, R.: Investigation of parasitic capacitances of In₂O₅Sn gate electrode recessed channel MOSFET for ULSI switching applications. *Microsyst. Technol.* **23**, 5867–5874 (2017)